Journal of Organometallic Chemistry xxx (2017) 1–9

Contents lists available at ScienceDirect

Journal of Organometallic Chemistry

journal homepage: www.elsevier.com/locate/jorganchem

Functionalized NHC-incorporated Te–Fe–Cu clusters: Facile synthesis, electrochemistry, and catalytic reaction

Minghuey Shieh*, Yu-Hsin Liu, Yu-Huei Li, Chien-Nan Lin, Chih-Chin Wang

Department of Chemistry, National Taiwan Normal University, Taipei 11677, Taiwan, Republic of China

ARTICLE INFO

Article history:
Received 26 September 2017
Received in revised form
26 October 2017
Accepted 28 October 2017
Available online xxx

This article is dedicated to Professor Irina P. Beletskaya for her outstanding contributions to the field of organometallic chemistry and catalysis.

Keywords:
Carbonyl
Catalysis
Electrochemistry
Heterometallic complexes
N-heterocyclic carbenes
Tellurium

ABSTRACT

Two novel $TeFe_3(CO)_9$-containing functionalized NHC dicopper complexes, $[TeFe_3(CO)_9\{Cu(Me_2\text{-bimy})\}_2]$ (**1**) and $[TeFe_3(CO)_9\{Cu(^iPr_2\text{-bimy})\}_2]$ (**2**), were prepared from the reaction of the ternary Te–Fe–Cu complex $[TeFe_3(CO)_9\{Cu(MeCN)\}_2]$ with bis-*N*-methyl- or bis-*N*-isopropyl-substituted benzimidazol-2-ylidene (Me_2-bimy or $^iPr_2$-bimy) under appropriate conditions, respectively. X-ray analysis showed that Me_2-bimy-introduced complex **1** displayed a $TeFe_3(CO)_9Cu(Me_2\text{-bimy})$ trigonal-bipyramidal core geometry having the Fe_2Cu face capped by a $Cu(Me_2\text{-bimy})$ fragment with the two bonded Cu atoms, whereas the bulkier $^iPr_2$-bimy-incorporated complex **2** exhibited a similar $TeFe_3(CO)_9Cu(^iPr_2\text{-bimy})$ core having the Fe_3 triangle coordinated by a $Cu(^iPr_2\text{-bimy})$ fragment with the two unbonded Cu atoms. On the other hand, when $[TeFe_3(CO)_9\{Cu(MeCN)\}_2]$ reacted with the 4,5-dichloro-substituted 1,3-dimethylimidazolium salt ($Me_2\text{-}Cl_2\text{-imy}\cdot HI$) in the presence of KO^tBu, a different type of $[TeFe_3(CO)_9\{Cu(Me_2\text{-}Cl_2\text{-imy})\}_2]$ (**3**) was produced in good yields. Cluster **3** was shown to possess a tetrahedral $TeFe_3$ core geometry in which the two Fe–Fe edges were each bridged by a $Cu(Me_2\text{-}Cl_2\text{-imy})$ group. According to solid-state packings, complex **1** revealed a cluster-based 3D-supramolecular framework and complexes **2** and **3** each formed a 1D-supramolecular chain, which was stabilized by intermolecular $C\text{–}H\cdots O$ interactions between COs and CH moieties of the corresponding NHC ligands. Further, these di-Cu(I) based complexes **1**–**3** exhibited catalytic activities toward the homocoupling of arylboronic acid with high yields. Importantly, the catalytic efficiencies of this series of functionalized NHC-incorporated $TeFe_3(CO)_9Cu_2$-based complexes perfectly paralleled the ease of their first oxidation and the greater electron density of the carbene atom in the NHC ligands, which was elucidated by electrochemistry, ^{13}C NMR, and DFT calculations.

© 2017 Elsevier B.V. All rights reserved.

1. Introduction

Heterometallic carbonyl clusters have attracted increased attention in recent years because of their structural versatility [1,2] and numerous applications in catalysts [3], magnetism [4], and nanotechnology [5]. The incorporation of chalcogenide ligands into heterometallic systems can help to stabilize the resulting clusters and harmonize their chemical and physical properties [1,2,6]. Among these studies, mixed Fe–Cu-containing chalcogenide carbonylates have been exploited because of their special properties [7–9]. In our previous studies, a family of E–Fe–Cu carbonyl complexes (E = S, Se, Te) which exhibited rich electrochemical properties were produced from reactions of the tetrahedral clusters $[EFe_3(CO)_9]^{2-}$ (E = S, Se, Te) with CuX (X = Cl, Br, I) or other Cu^+ reagents [7a,7b,7c]. Further, bisphosphine-bridged SFe_3Cu_2-based clusters and dipyridyl linkers-linked $TeFe_3Cu_2$-based polymers have also been reported to be potential semiconductors with ultra-narrow band gaps [8,9].

Until recently, $TeFe_3(CO)_9Cu_2$-incroporated *N*-heterocyclic carbene (NHC) complexes have been synthesized, and this type of the *N*-alkyl-substituted imidazole-2-ylidene (imy)-introduced Fe–Cu complexes exhibited pronounced catalytic activities toward the homocoupling of arylboronic acids [10]. Although it has been reported that precious metals, Pd [11,12], Rh [11,13], and Au [11,14], showed good catalytic activities for Suzuki homocoupling reactions, these catalytic systems typically require additional additives or ligands for success. Hence, the employment of ternary Te–Fe–Cu NHC catalysts for use in the homocoupling reactions with comparably high catalytic yields but without the need for additives, has attracted our continued research interest.

---

* Corresponding author.
E-mail address: mshieh@ntnu.edu.tw (M. Shieh).

https://doi.org/10.1016/j.jorganchem.2017.10.039
0022-328X/© 2017 Elsevier B.V. All rights reserved.

While the effect of the cluster $[TeFe_3(CO)_9]^{2-}$ as an effective ligand in these Te–Fe–Cu NHC catalysts has been studied [10], the cooperative effect of the NHC ligands and the $TeFe_3Cu_2$ core of these catalysts has remained unclear. Prompted by these facts, we attempted to synthesize new functionalized NHC-containing $TeFe_3Cu_2$-based complexes to systemically study the role of NHC ligands and the $TeFe_3Cu_2$ cluster in the Suzuki homocoupling reaction. In the present study, we have synthesized three different types of functionalized NHC-containing $TeFe_3Cu_2$-based complexes, i.e. structurally related bis-Me_2-bimy- and bis-$^iPr_2$-bimy-incorporated $TeFe_3(CO)_9Cu_2$-based clusters $[TeFe_3(CO)_9\{Cu(Me_2\text{-bimy})\}_2]$ (**1**) and $[TeFe_3(CO)_9\{Cu(^iPr_2\text{-bimy})\}_2]$ (**2**) (Me_2-bimy = 1,3-dimethylbenzimidazol-2-ylidene; $^iPr_2$-bimy = 1,3-diisopropylbenzimidazol-2-ylidene), and a bis-Cu(Me_2-Cl_2-imy)-bridged $TeFe_3$ cluster $[TeFe_3(CO)_9\{Cu(Me_2\text{-}Cl_2\text{-imy})\}_2]$ (**3**) (Me_2-Cl_2-imy = 1,3-dimethyl-4,5-dichloroimidazol-2-ylidene). Complexes **1**–**3** can be used as the $TeFe_3(CO)_9$-NHC-probed Cu(I) catalysts in the homocoupling of arylboronic acid with high catalytic yields. Furthermore, their catalytic efficiencies were also investigated and correlated with the electronic and steric effects of the $TeFe_3(CO)_9$ and functionalized NHC, as elucidated by electrochemistry, ^{13}C NMR, and DFT calculations.

2. Results and discussion

2.1. *Syntheses of bis-Me_2-bimy and bis-$^iPr_2$-bimy-incorporated $TeFe_3Cu_2$-based clusters and bis-Cu(Me_2-Cl_2-imy)-bridged $TeFe_3$-based cluster*

When the neutral Te–Fe–Cu cluster $[TeFe_3(CO)_9\{Cu(MeCN)\}_2]$ [8a] was treated with two equivalents of *in situ* generated 1,3-dimethylbenzimidazol-2-ylidene (Me_2-bimy) or 1,3-diisopropylbenzimidazol-2-ylidene ($^iPr_2$-bimy) by the deprotonation of the corresponding imidazolium salts with KO^tBu in THF solution at 0 °C and room temperature, $[TeFe_3(CO)_9\{Cu(Me_2\text{-bimy})\}_2]$ (**1**) and $[TeFe_3(CO)_9\{Cu(^iPr_2\text{-bimy})_2]$ (**2**) were produced in moderate yields, respectively (Scheme 1). Complexes **1** and **2** were fully characterized by spectroscopic methods and single-crystal X-ray diffraction analysis, and the ORTEP diagrams were plotted in Figs. 1 and 2. Both complexes **1** and **2** had a distorted $TeFe_3(CO)_9Cu$ trigonal-bipyramidal core geometry with a $TeFe_2$ ring residing in the equatorial plane, in which the triangular Fe_2Cu plane of **1** or the Fe_3 plane of **2** was further capped by one copper atom, where the two Cu atoms were each coordinated by a Me_2-bimy or $^iPr_2$-bimy fragment, respectively (Figs. 1 and 2). It is noteworthy that the covalently bonded Cu atoms in complex **1** were four- and five-coordinated, while both of the Cu atoms in complex **2** were four-coordinated, due to the greater steric hindrance of the *N*-isopropyl group, compared with *N*-methyl substituents, which caused Cu–Cu bond breakage in complex **2** (Figs. 1 and 2).

Further, the di-Cu(Me_2-Cl_2-imy)-bridged $TeFe_3$ cluster $[TeFe_3(CO)_9\{Cu(Me_2\text{-}Cl_2\text{-imy})\}_2]$ (**3**) was obtained from the one-pot reaction of $[TeFe_3(CO)_9\{Cu(MeCN)\}_2]$, 1,3-dimethyl-4,5-dichloroimidazolium iodide (Me_2-Cl_2-imy·HI), and KO^tBu in a ratio of 1: 2: 2 in THF solution (Scheme 1). As depicted in Fig. 3, complex **3** displayed a $TeFe_3(CO)_9$ tetrahedral geometry with two Fe–Fe edges each bridged by a Cu(Me_2-Cl_2-imy) group, in which two Cu(Me_2-Cl_2-imy) fragments sat in a *cis* orientation. According to a search of the Cambridge Crystallographic Data Centre, complexes **1**–**3** represent the first examples of benzimidazol-2-ylidene- or 4,5-dichloroimidazol-2-ylidene-containing mixed-metal carbonyl chalcogenide clusters. These results demonstrate that the ternary $TeFe_3Cu_2$-based clusters remained intact to tolerate these functionalized NHCs, forming a series of novel Te–Fe–Cu NHC complexes.

To further investigate the electronic properties of these functionalized NHC-containing Te–Fe–Cu clusters, ^{13}C nuclear magnetic resonance (NMR) of these complexes were carried out. The resonance of the carbene atoms in complexes **1**–**3** was found at 187.45, 183.83, and 180.28, respectively, in which the upfield-shift was observed from **1** to **2** and to **3**, indicating the trend of the increasing electron density of the carbene atom was from **1** to **2** and to **3**.

2.2. *X-ray structure comparison of **1**–**3***

According to single-crystal X-ray analysis, the benzimidazol-2-ylidene-incorporated complex **1** is structurally similar to the reported imidazol-2-ylidene-containing complex $[TeFe_3(CO)_9\{Cu(Me_2\text{-imy})\}_2]$ [10], both consisted of a $TeFe_3(CO)_9Cu$ core with a Fe_2Cu plane capped by a copper atom, where two Cu atoms each were linked by a Me_2-bimy or Me_2-imy ligand, respectively. The Cu–Cu bond in complex **1** (2.8747(8) Å) was significantly longer than that of $[TeFe_3(CO)_9\{Cu(Me_2\text{-imy})\}_2]$ (2.5949(9) Å) [10], due to the greater steric hindrance of the Me_2-bimy group compared with the Me_2-imy group (Table 1). As shown in Fig. 2, complex **2** can be viewed to possess a $TeFe_3(CO)_9$ tetrahedral core with $TeFe_2$ and Fe_3 faces each capped by a Cu($^iPr_2$-bimy) unit, with a mirror plane through the Te1, Fe2, Cu1, and Cu2 atoms, to give a Chinese gold ingot-like conformation. In addition, complex **3** had a comparatively open structure to display a bis-μ_2-Cu(Me_2-Cl_2-imy)-bridged tetrahedral $TeFe_3(CO)_9$ geometry. Notably, both Cu atoms in complex **2** were four-coordinated but severely distorted from the ideal tetrahedral geometry (56.448(9)°–147.13(1)°), while the two Cu atoms in complex **3** each were three-coordinated and formed a nearly ideal isosceles triangle with the associated Fe atoms and the carbene atom (Figs. 2 and 3 and Table S1). Addition to the known bonding type of complex **1**, the bis-μ_3-Cu($^iPr_2$-bimy)-containing complex **2** and the bis-μ_2-Cu(Me_2-Cl_2-imy)-bridged complex **3** represent new bonding modes in this Te–Fe–Cu NHC system, which are electronically and sterically influenced by the introduction of the functionalized NHC ligands, benzimidazol-2-ylidene or 4,5-dichloroimidazol-2-ylidene.

In complexes **1**–**3**, the copper atoms are close to the carbon atoms of adjacent COs and the corresponding Fe–C–O angles are bent slightly from 180°, which could form the weak Cu···C interactions (Figs. 1–3). Furthermore, the average $Cu–C_{carbene}$ bond of complexes **1**–**3** was within the range of the $Cu–C_{carbene}$ bonds (*ca.* 1.80–2.20 Å) in the reported Cu(I)-NHC complexes [10,15]. Importantly, in the solid-state packing, adjacent molecules of complex **1** are sufficiently close to form a three-dimensional network owing to the C–H···O hydrogen bonds [16] between COs and NHCs (Fig. S1 and Table S2). Further, the one-dimensional zigzag chain and chain-like structures of complexes **2** and **3** were revealed in their solid-state packings, respectively, also via C–H···O hydrogen bonds [16] between the COs and the corresponding NHC ligands (Fig. S2 and Table S2). These weak interactions may be an important factor in stabilizing these functionalized NHC-incorporated Te–Fe–Cu complexes in the solid state.

2.3. *Computational studies*

To investigate the differences in the electronic structures among these NHC-introduced Te–Fe–Cu-based complexes **1**–**3** and their parent complex $[TeFe_3(CO)_9\{Cu(MeCN)\}_2]$, density functional theory (DFT) calculations were performed at the B3PW91/def2-TZVP level [17]. The computational details are summarized in Table 2 and Tables S4–S9 as well as in Fig. 4.

As shown in Table 2, the natural charge of the $TeFe_3(CO)_9Cu_2$ cores in complexes **1**–**3** (**1**, −0.339; **2**, −0.327; **3**, −0.343) became

Please cite this article in press as: M. Shieh, et al., Journal of Organometallic Chemistry (2017), https://doi.org/10.1016/j.jorganchem.2017.10.039

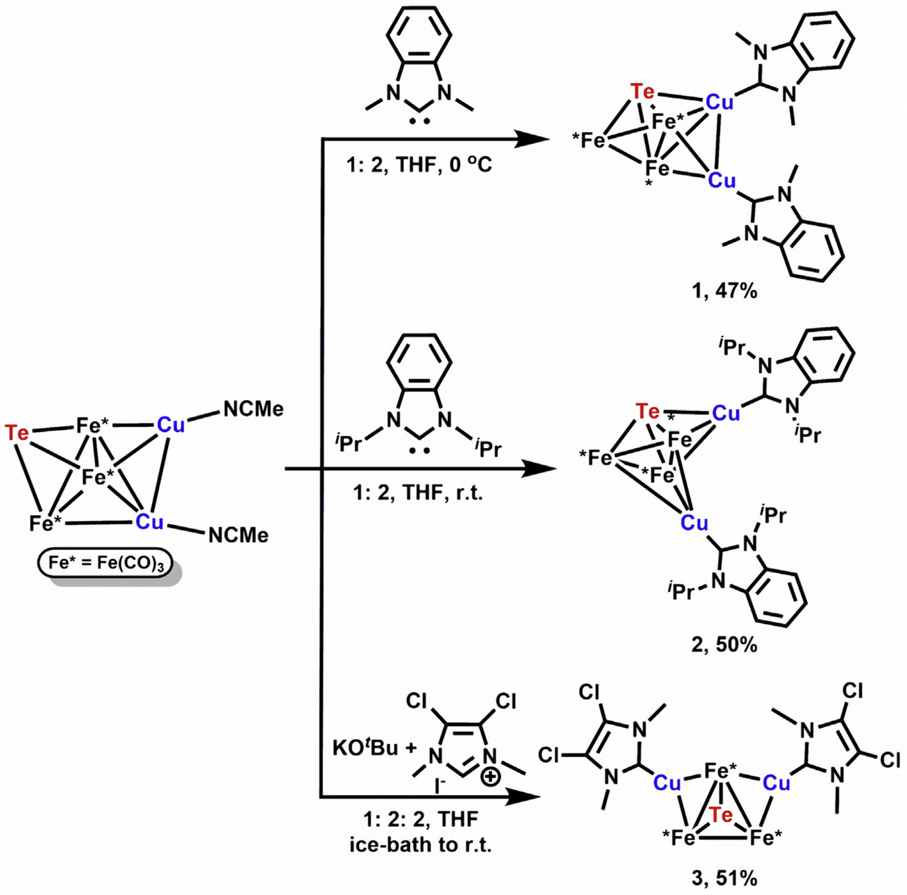

Scheme 1. Synthesis of functionalized NHC-containing Te–Fe–Cu carbonyl complexes **1**–**3**.

more negatively charged than that of [$TeFe_3(CO)_9\{Cu(MeCN)\}_2$] (−0.072), revealing the accumulated electron density of $TeFe_3(CO)_9Cu_2$ cores caused by the introduced NHC ligands. Moreover, the average natural charge of the Cu atoms in complexes **1**–**3** (**1**, 0.612; **2**, 0.638; **3**, 0.642) were also more negatively charged compared with that of [$TeFe_3(CO)_9\{Cu(MeCN)\}_2$] (0.683), implying that the Cu(I) centers in complexes **1**–**3** would be easily oxidized, which could facilitate their participation in oxidative addition in the catalytic reactions.

2.4. Electrochemistry

In view of the ligand effects of these Me_2-bimy, ^{i}Pr_2-bimy, and Me_2-Cl_2-imy incorporated $TeFe_3Cu_2$-based complexes, their electrochemical behaviors were examined by differential pulse voltammetry (DPV) in MeCN under N_2, which was further compared with their related complex [$TeFe_3(CO)_9\{Cu(Me_2\text{-imy})\}_2$] [10]. Because of the reported one-electron oxidation of Cu(I) (0.45–0.36 V) [18] and the irreversible desorption of Cu (−0.33 to −0.38 V) [19], the DPV profiles of complexes **1**, **2**, and **3** are only discussed between 0.30 and −0.20 V. For the DPV measurements, the electron stoichiometry is determined by the measurement of the peak width at half-height ($W_{1/2}$) [20]. The DPV data are summarized in Table S3 and are plotted in Fig. 5, respectively.

As shown in Fig. 5 and Table S3, the DPV studies revealed that complexes **1**–**3** and [$TeFe_3(CO)_9\{Cu(Me_2\text{-imy})\}_2$] [10] each exhibited one quasi-reversible reduction and two quasi-reversible oxidations. These results indicate that complexes **1**–**3** and related [$TeFe_3(CO)_9\{Cu(Me_2\text{-imy})\}_2$] show similar types of redox patterns, with three redox potentials, resulting from a similar distribution of their HOMO and LUMO each of which received significant contributions from the d orbitals of Te and Fe atoms and the p and d orbitals of the Cu atoms (Figs. 4 and 5 and Table S4). As a consequence, these reduction and oxidations mainly occurred in the $TeFe_3(CO)_9Cu_2$ metal core. DPV further showed that the first oxidation potential of complex **3** (0.018 V) and [$TeFe_3(CO)_9\{Cu(Me_2\text{-imy})\}_2$] (0.015 V) was cathodically shifted compared with that of the *N*-methyl or *N*-isopropyl benzimidazol-2-ylidene-containing complex **1** (0.084 V) or **2** (0.072 V), indicating that the $TeFe_3(CO)_9Cu_2$ cores in complex **3** and [$TeFe_3(CO)_9\{Cu(Me_2\text{-imy})\}_2$] were more easily oxidized than those of complexes **1** and **2**.

2.5. Catalytic reaction

In order to further explore the behavior of complexes **1**–**3** in catalyzing Suzuki homocoupling reactions, complexes **1**–**3** were used to catalyze the homocoupling of 4-bromophenylboronic acid under conditions that included a Cu loading of 1.0 mol%, a methanol solvent system, an atmosphere of O_2, room temperature, and with no additives such as bases, ligands, or other oxidants (Table 3). As shown in Table 3, complexes **1**–**3** (entries 1–3) all exhibited excellent catalytic yields (**1**, 82%, 4.5 h; **2**, 80%, 3 h; **3**, 81%, 2.2 h). These results indicate that our synthesized functionalized NHC $TeFe_3Cu_2$-based complexes could serve as effective catalysts for the homocoupling of arylboronic acids.

For comparison, the benzimidazol-2-ylidene-incorporated complex **1** (82%) had a similar yield with the structurally analogous [$TeFe_3(CO)_9\{Cu(Me_2\text{-imy})\}_2$] (88%) but a lower turnover frequency

Please cite this article in press as: M. Shieh, et al., Journal of Organometallic Chemistry (2017), https://doi.org/10.1016/j.jorganchem.2017.10.039

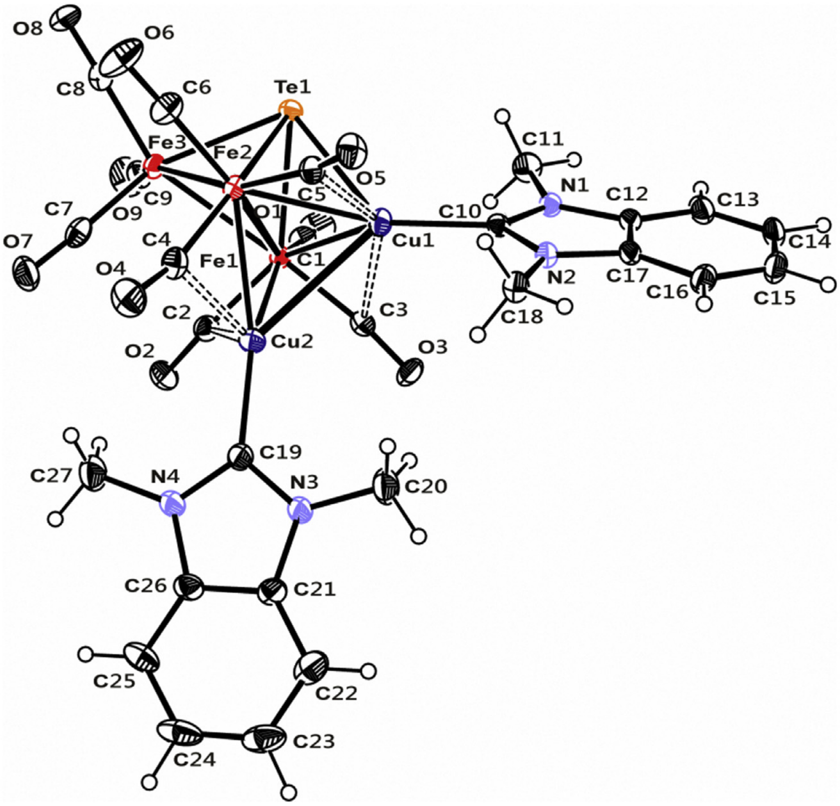

Fig. 1. ORTEP diagram (30% thermal ellipsoids) showing the structure and atom labeling for **1**.

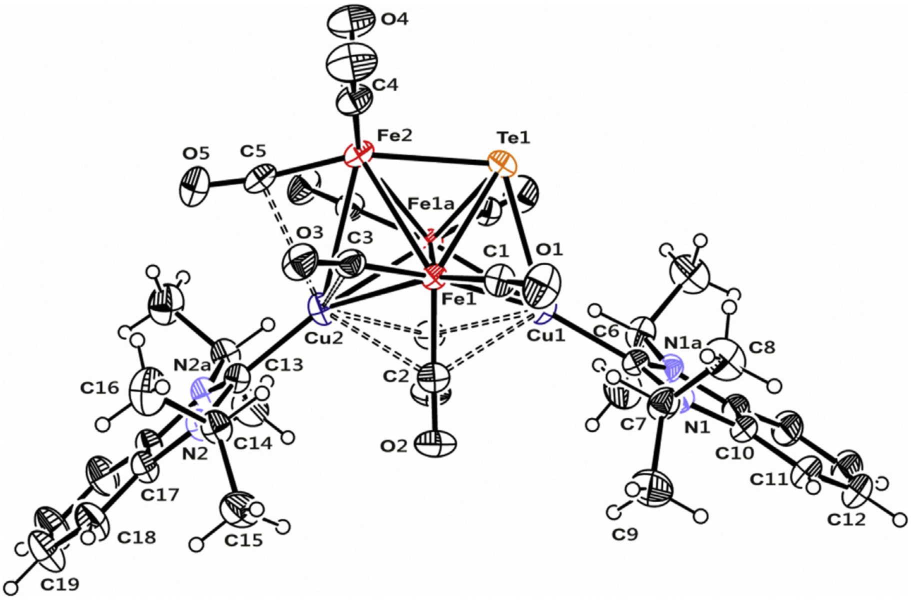

Fig. 2. ORTEP diagram (30% thermal ellipsoids) showing the structure and atom labeling for **2**. Atoms with an additional label a are at the equivalent positions (x, 0.5−y, z).

(TOF) than that of [$TeFe_3(CO)_9\{Cu(Me_2$-imy$)\}_2$], showing that presence of benzyl-decorated NHC ligands slightly retard the catalytic reaction. In addition, while they showed similar turnover numbers (TONs), the *N*-isopropyl-substituted complex **2** turned out to have a higher TOF than that of the *N*-methyl-substituted complex **1**, due to the steric effect of the N-substituents. It should also be noted that the TOF of the 4,5-dichloroimidazol-2-ylidene-containing complex **3** was significantly higher than those of the benzimidazol-2-ylidene-incorporated complexes **1** and **2**, suggesting that the less hindered Cu centers in complex **3** could possibly facilitate the transmetallation with arylboronic acid via a proposed Cu(I)/Cu(III) catalytic cycle [21]. Importantly, the catalytic efficiencies of complexes **1**–**3** and [$TeFe_3(CO)_9\{Cu(Me_2$-imy$)\}_2$] were found to perfectly parallel the ease of their first oxidation

Please cite this article in press as: M. Shieh, et al., Journal of Organometallic Chemistry (2017), https://doi.org/10.1016/j.jorganchem.2017.10.039

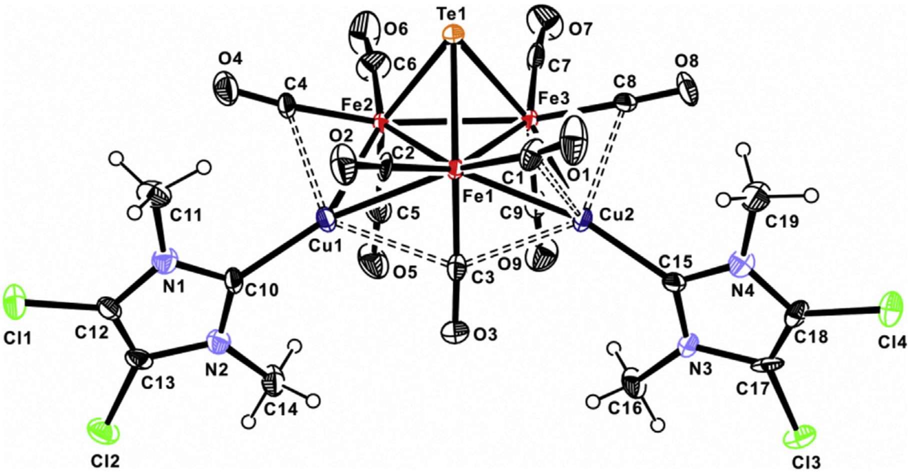

Fig. 3. ORTEP diagram (30% thermal ellipsoids) showing the structure and atom labeling for **3**. Only the major disordered configuration is shown.

Table 1
Selected bond distances (Å) of **1**, **2**, **3**, and related complexes.

Complex	Te–Fe[b]	Fe–Fe[b]	Fe–Cu[b]	Cu–Cu	Cu–X	Te–Cu	Ref
1 (X = C)	2.51(1)	2.7(1)	2.53(2)	2.8747(8)	1.941(4)[c,f] 1.955(5)[d,g]	2.7435(6)	a
2 (X = C)	2.513(6)	2.70(5)	2.6(1)		1.928(4)[d,f] 1.965(4)[d,h]	2.7237(6)	a
3 (X = C)	2.48(2)	2.70(3)	2.51(3)		1.95(1)[b,e]		a
$[TeFe_3(CO)_9\{Cu(MeCN)\}_2]$ (X = N)	2.486(3)	2.75(5)	2.52(5)	2.605(1)	1.940(6)[c,h] 1.918(6)[d,g]		[8a]
$[TeFe_3(CO)_9\{Cu(Me_2\text{-imy})\}_2]$ (X = C)	2.506(7)	2.68(6)	2.56(6)	2.5949(9)	1.936(6)[c,f] 1.928(6)[d,g]	2.7818(7)	[10]

[a] This work.
[b] Average bond distances.
[c] Five-coordinated Cu atom.
[d] Four-coordinated Cu atom.
[e] Three-coordinated Cu atom.
[f] The Cu-NHC fragment capped the $TeFe_2$ triangle.
[g] The Cu-NHC fragment capped the Fe_2Cu triangle.
[h] The Cu-NHC fragment capped the Fe_3 triangle.

Table 2
Results of natural population analyses of **1**, **2**, **3**, and related complexes.

Complex	Natural charge			
	Te	Fe[a]	Cu[a]	$TeFe_3(CO)_9Cu_2$
1	0.283	−0.627	0.612	−0.339
2	0.449	−0.600	0.638	−0.327
3	0.570	−0.361	0.642	−0.343
$[TeFe_3(CO)_9\{Cu\ (MeCN)\}_2]$	0.505	−0.541	0.683	−0.072
$[TeFe_3(CO)_9\{Cu(Me_2\text{-imy})\}_2]$	0.403	−0.520	0.608	−0.343

[a] Average natural charge.

potentials, demonstrating that the catalyst activities of these complexes were correlated with the resultant electron density of the $TeFe_3Cu_2$ core, which was influenced by the incoming NHC ligands (Table 3 and Fig. 5). Moreover, their catalytic efficiencies can also be probed by the ^{13}C shift of the carbene atoms and the findings indicate that the larger electron density of the carbene atoms could aid in stabilizing the unstable Cu(III) intermediate in the homocoupling of arylboronic acid.

3. Conclusions

In conclusion, three different types of functionalized NHC-containing Te–Fe–Cu complexes **1**–**3** have been synthesized, including Me_2-bimy- and $^iPr_2$-bimy-incorporated $TeFe_3Cu_2$-based or Me_2-Cl_2-imy-bridged $TeFe_3$-based clusters. In their solid-state packings, complex **1** revealed a cluster-based 3D network and complexes **2** and **3** each displayed a 1D-supramolecular chain, which was sustained by C–H···O interactions. In addition, these di-Cu(I) based complexes **1**–**3** exhibited effectively catalytic activities with respect to the homocoupling of arylboronic acid. Importantly, the catalytic efficiencies of these resulting Te–Fe–Cu NHC catalysts were in perfect parallel with the ease of their first oxidation and the greater electron density of the carbene atom in these NHC ligands. Finally, this work provided a facile approach for evaluating the catalytic activities of these Te–Fe–Cu NHC catalysts for the homocoupling reaction of arylboronic acid in terms of the comparison of their oxidation potentials and the chemical shifts of the carbene atoms.

4. Experimental section

4.1. General methods

All reactions were performed under an atmosphere of pure nitrogen using standard Schlenk techniques [22]. Solvents were purified, dried, and distilled under nitrogen prior to use. KO^tBu (ACROS) and 4-bromophenylboronic acid (Lancaster) were used as

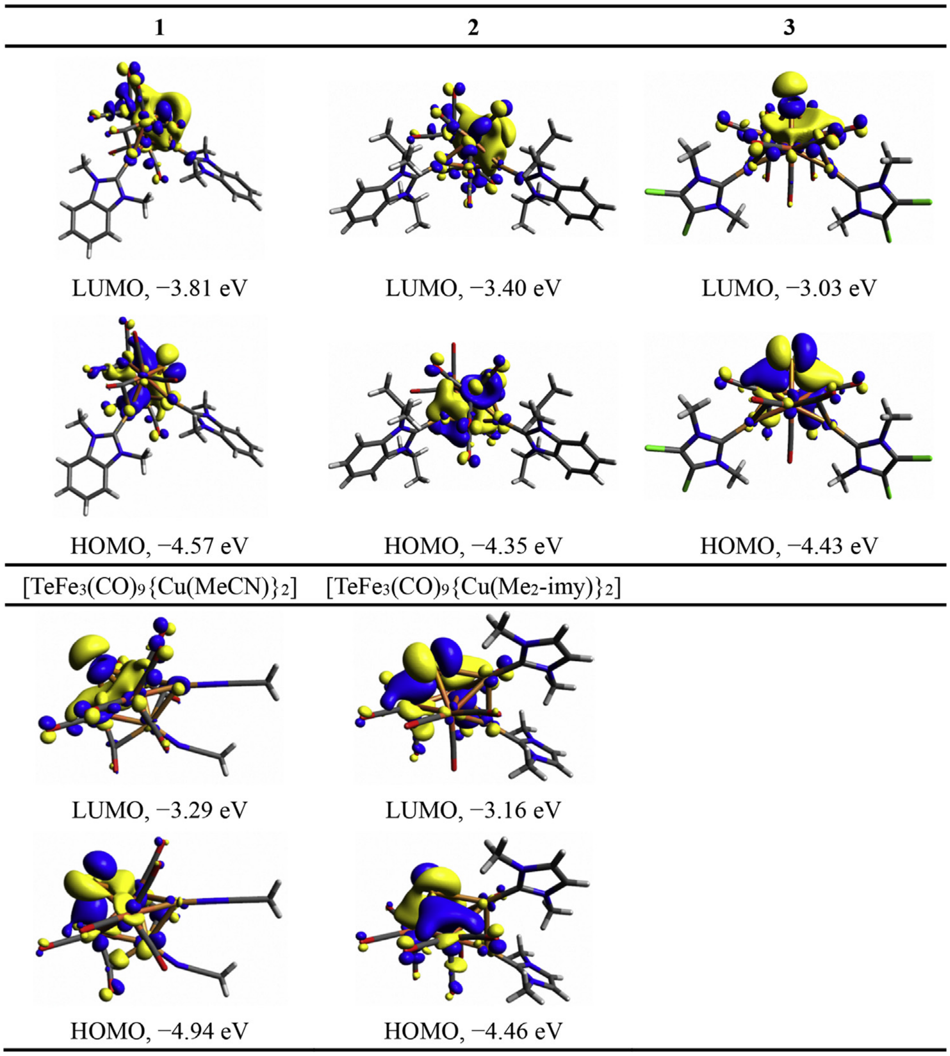

Fig. 4. The spatial graphs (isovalue = 0.03–0.04) of the frontier molecular orbitals and their associated calculated energies of **1**–**3**, [TeFe$_3$(CO)$_9${Cu(MeCN)}$_2$], and [TeFe$_3$(CO)$_9${Cu(Me$_2$-imy)}$_2$].

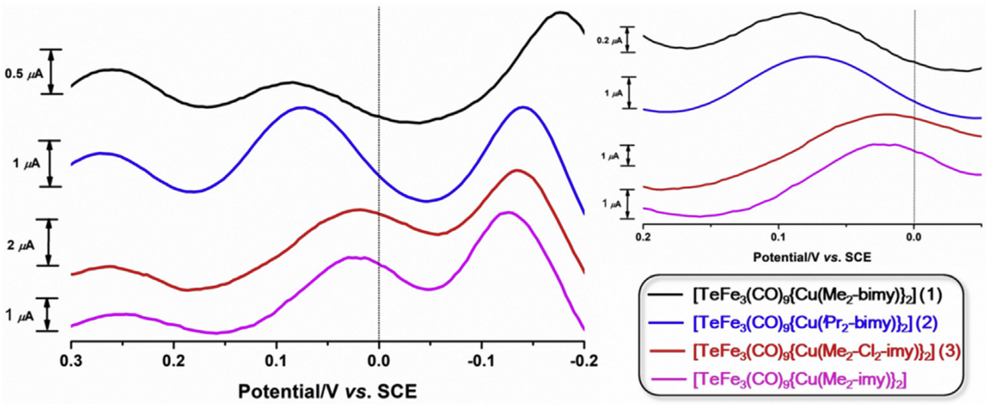

Fig. 5. DPV in MeCN of **1**–**3** and [TeFe$_3$(CO)$_9${Cu(Me$_2$-imy)}$_2$]. Conditions: electrolyte, 0.1 M Bu$_4$NClO$_4$; working electrode, glassy carbon; scan rate, 100 mV/s. Potentials are vs. SCE. The inset shows the first one-electron quasi-reversible oxidation between −0.05 and 0.20 V *vs.* SCE.

received. [Et$_4$N]$_2$[TeFe$_3$(CO)$_9$] [23], [Cu(MeCN)$_4$][BF$_4$] [24], [TeFe$_3$(CO)$_9${Cu(MeCN)}$_2$] [8a], and the imidazolium salts, 1,3-dimethylbenzimidazolium iodide (Me$_2$-bimy·HI) [25a], 1,3-diisopropylbenzimidazolium iodide (^{i}Pr$_2$-bimy·HI) [25b], and 1,3-dimethyl-4,5-dichloro-imidazolium iodide (Me$_2$-Cl$_2$-imy·HI) [25c], were prepared according to the previously published

Please cite this article in press as: M. Shieh, et al., Journal of Organometallic Chemistry (2017), https://doi.org/10.1016/j.jorganchem.2017.10.039

Table 3
Homocoupling of 4-bromophenylboronic acid with different catalysts.[a]

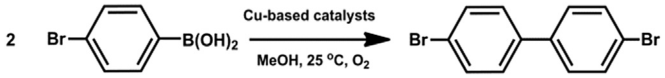

Entry	Catalyst	Cu (mol%)	Time (h)	Yield (%)[b,c]	TON[d]	TOF (h^{-1})[e]	Ref.
1	$[TeFe_3(CO)_9\{Cu(Me_2\text{-bimy})\}_2]$ (**1**)	1.0	4.5	82	82	18.2	f
2	$[TeFe_3(CO)_9\{Cu(^iPr_2\text{-bimy})\}_2]$ (**2**)	1.0	3	80	80	26.7	f
3	$[TeFe_3(CO)_9\{Cu(Me_2\text{-}Cl_2\text{-imy})\}_2]$ (**3**)	1.0	2.2	81	81	36.8	f
4	$[TeFe_3(CO)_9\{Cu(Me_2\text{-imy})\}_2]$	1.0	2	88	88	44.0	[10]

[a] Reaction conditions: 4-bromophenylboronic acid (1.0 mmol), MeOH (3.0 mL), 25 °C, O_2 (1 atm, balloon).
[b] The isolated yield as an average of three runs.
[c] All reactions were monitored by TLC.
[d] Turnover number per copper for the 4-bromophenylboronic acid consumed.
[e] TON per hour.
[f] This work.

methods. Compounds were purified by chromatography on Merck 60 silica gel (40–63 μm) and analytical thin layer chromatography (TLC) was performed on Silica Gel 60 F254 precoated plates. Infrared spectra were recorded on a Perkin-Elmer Paragon 1000 IR spectrometer. The NMR spectra were obtained on a Bruker AV 400 at 400.13 MHz for ^{1}H and 100.61 MHz for ^{13}C or on a Bruker AV 500 at 500.13 MHz for ^{1}H and 125.76 MHz for ^{13}C. ^{1}H and ^{13}C chemical shifts are reported in parts per million and were calibrated relative to DMSO-d_5 (^{1}H: 2.49 ppm, ^{13}C: 39.51 ppm) as the internal standard. Elemental analyses for C, H, and N were performed on a Perkin-Elmer 2400 analyzer at the MOST Regional Instrumental Center at National Taiwan University, Taipei, Taiwan.

4.2. *Synthesis of $[TeFe_3(CO)_9\{Cu(Me_2\text{-bimy})\}_2]$ (**1**)*

A 20 mL of freshly dried THF was added to a mixture of Me_2-bimy·HI (0.40 g, 1.46 mmol) and KO^{t}Bu (0.13 g, 1.17 mmol), and the mixture was stirred in an ice-water bath for 2 h. The resulting dark yellow solution was filtered and removed under vacuum. The residue was washed with *n*-hexane several times and then 1,3-dimethylbenzimidazol-2-ylidene (Me_2-bimy) was obtained (0.10 g, 0.68 mmol). A 15 mL THF was added to a mixture of $[TeFe_3(CO)_9\{Cu(MeCN)\}_2]$ (0.26 g, 0.34 mmol) and Me_2-bimy (0.10 g, 0.68 mmol) in an ice-water bath, which was stirred for 15 min. The resulting solution was filtered, and the solvent was removed under vacuum. The residue was washed with deionized water and *n*-hexane several times and then extracted with Et_2O to give a purplish-brown solution which was recrystallized with Et_2O/CH_2Cl_2 to give $[TeFe_3(CO)_9\{Cu(Me_2\text{-bimy})\}_2]$ (**1**) as a purplish-black solid (0.154 g, 0.159 mmol, 47% based on $[TeFe_3(CO)_9\{Cu(MeCN)\}_2]$). IR ($\nu_{CO}$, CH_2Cl_2): 2033 (m), 1976 (vs), 1920 (m), 1875 (w) cm^{-1}. ^{1}H NMR (500 MHz, DMSO-d_6, 300 K, ppm): δ 7.69 (dd, 4H, Ar-*H*), 7.43 (dd, 4H, Ar-*H*), 4.02 (s, 12H; C*H*$_3$). ^{13}C NMR (125 MHz, DMSO-d_6, 300 K, ppm): δ 219.07 (Fe-*C*O), 187.45 ($C_{carbene}$), 133.11, 123.29, 111.15 (Ar-*C*), 34.32 (*C*H$_3$). Anal. Calcd for $C_{27}H_{20}Cu_2Fe_3N_4O_9Te$: C, 33.55; H, 5.80; N, 2.09. Found: C, 33.65; H, 5.78; N, 2.44. Mp: 97 °C dec. Crystals of **1** suitable for X-ray diffraction were grown from Et_2O/CH_2Cl_2.

4.3. *Synthesis of $[TeFe_3(CO)_9\{Cu(^iPr_2\text{-bimy})\}_2]$ (**2**)*

A 15 mL of freshly dried THF was added to a mixture of $^iPr_2$-bimy·HI (0.22 g, 0.68 mmol) and KO^{t}Bu (0.076 g, 0.68 mmol), and the mixture was stirred in an ice-water bath for 1 h. The resulting solution was filtered, and the creamy white filtrate was then transferred to 15 mL of a THF solution of $[TeFe_3(CO)_9\{Cu(MeCN)\}_2]$ (0.26 g, 0.34 mmol) and the resulting solution was stirred for another 1 h. The resulting solution was filtered, and the solvent was removed under vacuum. The residue was washed with deionized water and *n*-hexane several times and then extracted with CH_2Cl_2 to give a purplish-brown solution which was recrystallized with *n*-hexane/Et_2O/CH_2Cl_2 to give $[TeFe_3(CO)_9\{Cu(^iPr_2\text{-bimy})\}_2]$ (**2**) as a purplish-black solid (0.15 g, 0.17 mmol, 50% based on $[TeFe_3(CO)_9\{Cu(MeCN)\}_2]$). IR ($\nu_{CO}$, CH_2Cl_2): 2026 (m), 1973 (vs), 1922 (m) cm^{-1}. ^{1}H NMR (500 MHz, DMSO-d_6, 300 K, ppm): δ 7.87 (dd, 4H, Ar-*H*), 7.38 (dd, 4H, Ar-*H*), 5.17 (m, 4H, NC*H*(CH$_3$)$_2$), 1.67 (d, 24H, NCH(C*H*$_3$)$_2$). ^{13}C NMR (125 MHz, DMSO-d_6, 300 K, ppm): δ 219.19 (Fe-*C*O), 183.83 ($C_{carbene}$), 132.26, 123.33, 112.71 (Ar-*C*), 51.92 (N*C*H(CH$_3$)$_2$), 21.95 (NCH(*C*H$_3$)$_2$). Anal. Calcd for $C_{35}H_{36}Cu_2Fe_3N_4O_9Te$: C, 38.90; H, 3.36; N, 5.19. Found: C, 38.67; H, 3.49; N, 5.45. Mp: 67 °C dec. Crystals of **2** suitable for X-ray diffraction were grown from *n*-hexane/Et_2O/CH_2Cl_2.

4.4. *Synthesis of $[TeFe_3(CO)_9\{Cu(Me_2\text{-}Cl_2\text{-imy})\}_2]$ (**3**)*

A mixture of $[TeFe_3(CO)_9Cu_2(MeCN)_2]$ (0.35 g, 0.47 mmol), Me_2-Cl_2-Imy·HI (0.28 g, 0.94 mmol), and KO^{t}Bu (0.10 g, 0.93 mmol) was dissolved in a 20 mL of freshly dried THF and the resulting solution stirred in an ice-water bath for 6 h. The resulting solution was filtered, and the solvent was removed under vacuum. The residue was washed with deionized water and *n*-hexane several times and then extracted with CH_2Cl_2 to give a purplish-brown solution which was recrystallized from *n*-hexane/Et_2O/CH_2Cl_2 to give $[TeFe_3(CO)_9\{Cu(Me_2\text{-}Cl_2\text{-imy})\}_2]$ (**3**) as a purplish-black solid (0.24 g, 0.24 mmol, 51% based on $[TeFe_3(CO)_9\{Cu(MeCN)\}_2]$). IR ($\nu_{CO}$, CH_2Cl_2): 2022 (m), 1977 (vs), 1894 (w) cm^{-1}. ^{1}H NMR (500 MHz, DMSO-d_6, 300 K, ppm): δ 3.79 (s, 6 H, NC*H*$_3$). ^{13}C NMR (125 MHz, DMSO-d_6, 300 K, ppm): δ 218.86 (Fe-*C*O), 180.28 ($C_{carbene}$), 115.99 (*C*Cl), 36.32 (N*C*H$_3$). Anal. Calcd for $C_{19}H_{12}Cl_4Cu_2Fe_3N_4O_9Te$: C, 22.72; H, 1.20; N, 5.58. Found: C, 22.66; H, 1.27; N, 5.55. Mp: 102 °C dec. Crystals of **3** suitable for X-ray diffraction were grown from *n*-hexane/Et_2O/CH_2Cl_2.

4.5. *Homocoupling of 4-bromophenylboronic acid with catalysts **1**, **2**, and **3***

A 3 mL of MeOH solution of catalyst **1**, **2**, or **3** and 4-bromophenylboronic acid (1.00 mmol) was stirred at 25 °C in an

Please cite this article in press as: M. Shieh, et al., Journal of Organometallic Chemistry (2017), https://doi.org/10.1016/j.jorganchem.2017.10.039

O_2 atmosphere. After the reaction reached completion, which was determined by TLC to detect the disappearance of the starting material, 4-bromophenylboronic acid, the resulting reaction mixture was evaporated under vacuum. The residue was dissolved in CH_2Cl_2 and purified by column chromatography on silica gel using *n*-hexane as eluent to afford the biaryl product which was confirmed by NMR spectroscopy. To compare the productivities of all catalysts, all the homocoupling reactions quoted herein were carried out repeatedly and carefully to ensure accuracy.

4.6. X-ray structural determinations

Selected crystallographic parameters for **1**, **2**, and **3** are given in Table S10. The Selected distances and angles are listed in Table 1 and Table S1. All crystals were mounted on glass fibers with epoxy cement. Data collection for **1** and **2** were carried out on a Bruker Apex II CCD diffractometer with graphite-monochromated Mo Kα radiation at 200 K for **1** and 300 K for **2** in the 2θ range of 2.0–50° employing θ–2θ scans. Data collection of **3** was collected using a Bruker D8 Venture diffractometer with graphite-monochromated Mo Kα radiation at 200 K in the 2θ range of 2.0–50° employing θ–2θ scans. Empirical absorption correction of these complexes **1**–**3** based on the multi-scan method was applied using the program SADABS [26]. All structures were solved by the direct methods and difference Fourier maps and refined with SHELXL-97 package [27]. For complex **3**, the Te1, Fe1, Fe2, Fe3, Cu1, and Cu2 atoms were disordered with 90% occupancy and 10% for Te1′, Fe1′, Fe2′, Fe3′, Cu1′, and Cu2′, respectively, in which COs and NHC ligands for the minor component in the final electron density map were at the limits of resolution [28] (Fig. S3). The displacement parameters for C4 and C10 as well as C8 and C15 in complex **3** were constrained to equal amounts using an EADP constraint to obtain reasonable thermal parameters. All non-H atoms of **1**, **2**, and **3** were with anisotropic temperature factors. CCDC reference numbers 1570700 for **1**, 1570705 for **2**, and 1570706 for **3** contain the supplementary crystallographic data for this paper.

Acknowledgments

This work was supported by the Ministry of Science and Technology of Taiwan (Grant No. 104-2113-M-003-004-MY3 to M. Shieh). We wish to thank the NCHC of Taiwan for providing the computer time and the facilities. Our gratitude also goes to the Academic Paper Editing Clinic, NTNU.

Appendix A. Supplementary data

Supplementary data related to this article can be found at https://doi.org/10.1016/j.jorganchem.2017.10.039.

References

[1] (a) D.F. Shriver, H.D. Kaesz, R.D. Adams (Eds.), The Chemistry of Metal Cluster Complexes, Wiley-VCH Publishers, New York, 1990;
(b) P. Braunstein, L.A. Oro, P.R. Raithby (Eds.), Metal Clusters in Chemistry, Wiley-VCH Publishers, Weinheim, 1999.
[2] (a) P. Mathur, Adv. Organomet. Chem. 41 (1997) 243–314;
(b) N.A. Compton, R.J. Errington, N.C. Norman, Adv. Organomet. Chem. 31 (1990) 91–182;
(c) M.G. Richmond, Coord. Chem. Rev. 249 (2005) 2763–2786;
(d) M. Shieh, C.-Y. Miu, Y.-Y. Chu, C.-N. Lin, Coord. Chem. Rev. 256 (2012) 637–694.
[3] (a) S.C. Lee, R.H. Holm, Chem. Rev. 104 (2004) 1135–1157;
(b) P. Buchwalter, J. Rosé, P. Braunstein, Chem. Rev. 115 (2015) 28–126.
[4] (a) R.D. Adams, S. Miao, M.D. Smith, H. Farach, C.E. Webster, J. Manson, M.B. Hall, Inorg. Chem. 43 (2004) 2515–2525;
(b) A. Eichhöfer, J. Olkowska-Oetzel, D. Fenske, K. Fink, V. Mereacre, A.K. Powell, G. Buth, Inorg. Chem. 48 (2009) 8977–8984;
(c) M. Shieh, C.-H. Yu, Y.-Y. Chu, Y.-W. Guo, C.-Y. Huang, K.-J. Hsing, P.-C. Chen, C.-F. Lee, Chem. Asian J. 8 (2013) 963–973;
(d) M. Shieh, C.-N. Lin, C.-Y. Miu, M.-H. Hsu, Y.-W. Pan, L.-F. Ho, Inorg. Chem. 49 (2010) 8056–8066;
(e) M. Shieh, R.-L. Chung, C.-H. Yu, M.-H. Hsu, C.-H. Ho, S.-M. Peng, Y.-H. Liu, Inorg. Chem. 42 (2003) 5477–5479.
[5] (a) R. Ferrando, J. Jellinek, R.L. Johnston, Chem. Rev. 108 (2008) 845–910;
(b) C. Femoni, M.C. Iapalucci, G. Longoni, C. Tiozzo, S. Zacchini, Angew. Chem. Int. Ed. 47 (2008) 6666–6669;
(c) A. Naitabdi, O. Toulemonde, J.P. Bucher, J. Rosé, P. Braunstein, R. Welter, M. Drillon, Chem.–Eur. J. 14 (2008) 2355–2362;
(d) F. Schweyer-Tihay, C. Estournès, P. Braunstein, J. Guille, J.-L. Paillaud, M. Richard-Plouet, J. Rosé, Phys. Chem. Chem. Phys. 8 (2006) 4018–4028.
[6] (a) L.C. Roof, J.W. Kolis, Chem. Rev. 93 (1993) 1037–1080;
(b) K.H. Whitmire, Adv. Organomet. Chem. 42 (1998) 1–145.
[7] (a) M. Shieh, C.-Y. Miu, C.-J. Lee, W.-C. Chen, Y.-Y. Chu, H.-L. Chen, Inorg. Chem. 47 (2008) 11018–11031;
(b) B.-G. Chen, C.-H. Ho, C.-J. Lee, M. Shieh, Inorg. Chem. 48 (2009) 10757–10768;
(c) M. Shieh, C.-Y. Huang, C.-J. Lee, K.-J. Hsing, Y.-W. Li, Y.-Y. Chu, W.-T. Jhu, Polyhedron 52 (2013) 879–889;
(d) C.-Y. Miu, H.-H. Chi, S.-W. Chen, J.-J. Cherng, M.-H. Hsu, Y.-X. Huang, M. Shieh, New J. Chem. 35 (2011) 2442–2455;
(e) U. Jayarathne, S.R. Parmelee, N.P. Mankad, Inorg. Chem. 53 (2014) 7730–7737;
(f) R.D. Pergola, M. Bruschi, A. Sironi, M. Manassero, C. Manassero, D. Strumolo, S. Fedi, P. Zanello, Dalton Trans. 40 (2011) 5464–5475.
[8] (a) M. Shieh, C.-H. Ho, W.-S. Sheu, B.-G. Chen, Y.-Y. Chu, C.-Y. Miu, H.-L. Liu, C.-C. Shen, J. Am. Chem. Soc. 130 (2008) 14114–14116;
(b) M. Shieh, C.-C. Yu, C.-Y. Miu, C.-H. Kung, C.-Y. Huang, Y.-H. Liu, H.-L. Liu, C.-C. Shen, Chem.–Eur. J. 23 (2017) 11261–11271.
[9] C.-N. Lin, W.-T. Jhu, M. Shieh, Chem. Commun. 50 (2014) 1134–1136.
[10] C.-N. Lin, C.-Y. Huang, C.-C. Yu, Y.-M. Chen, W.-M. Ke, G.-J. Wang, G.-A. Lee, M. Shieh, Dalton Trans. 44 (2015) 16675–16679.
[11] R.N. Dhital, H. Sakurai, Asian J. Org. Chem. 3 (2014) 668–684 (and references therein).
[12] (a) A.R. Kapdi, G. Dhangar, J.L. Serrano, J.A. De Haro, P. Lozano, I.J.S. Fairlamb, RSC Adv. 4 (2014) 55305–55312 (and references therein);
(b) M. Guo, L. Qi, M. Lv, X. Zhou, H. Liang, S. Chen, Lett. Org. Chem. 12 (2015) 205–209;
(c) J. Xia, M. Cheng, Q. Chen, M. Cai, Appl. Organomet. Chem. 29 (2015) 113–116.
[13] T. Vogler, A. Studer, Adv. Synth. Catal. 350 (2008) 1963–1967 (and references therein).
[14] (a) K. Sharma, V. Bhalla, M. Kumar, RSC Adv 4 (2014) 53795–53800 (and reference therein);
(b) A. Monopoli, A. Afzal, C. Di Franco, N. Ditaranto, N. Cioffi, A. Nacci, P. Cotugno, L. Torsi, J. Mol. Catal. A Chem. 386 (2014) 101–107 (and reference therein);
(c) K.M. Parida, S. Singha, P.C. Sahoo, S. Sahu, J. Mol. Catal. A Chem. 342–343 (2011) 11–17.
[15] B. Liu, C. Chen, Y. Zhang, X. Liu, W. Chen, Organometallics 32 (2013) 5451–5460 (and references therein).
[16] (a) D. Braga, F. Grepioni, Acc. Chem. Res. 30 (1997) 81–87;
(b) D. Braga, F. Grepioni, K. Biradha, V.R. Pedireddi, G.R. Desiraju, J. Am. Chem. Soc. 117 (1995) 3156–3166.
[17] (a) A.D. Becke, J. Chem. Phys. 98 (1993) 5648–5652;
(b) J.P. Perdew, Y. Wang, Phys. Rev. B 45 (1992) 13244–13249;
(c) F. Weigend, R. Ahlrichs, Phys. Chem. Chem. Phys. 7 (2005) 3297–3305.
[18] (a) V.W.-W. Yam, W.-K. Lee, T.-F. Lai, Organometallics 12 (1993) 2383–2387;
(b) V.W.-W. Yam, W.-K. Lee, K.-K. Cheung, B. Crystall, D. Phillips, J. Chem. Soc. Dalton Trans. (1996) 3283–3287;
(c) V.W.-W. Yam, W.K.-M. Fung, M.-T. Wong, Organometallics 16 (1997) 1772–1778.
[19] (a) M. Scheer, A. Schindler, R. Merkle, B.P. Johnson, M. Linseis, R. Winter, C.E. Anson, A.V. Virovets, J. Am. Chem. Soc. 129 (2007) 13386–13387;
(b) X. Xue, X.-S. Wang, R.-G. Xiong, X.-Z. You, B.F. Abrahams, C.-M. Che, H.-X. Ju, Angew. Chem. Int. Ed. 41 (2002) 2944–2946;
(c) M.S. Doescher, J.M. Tour, A.M. Rawlett, M.L. Myrick, J. Phys. Chem. B 105 (2001) 105–110.
[20] (a) A.J. Bard, L.R. Faulkner, Electrochemical Methods: Fundamentals and Applications, second ed., John Wiley & Sons, New York, 2001, p. 291;
(b) T. Nakanishi, H. Murakami, T. Sagara, N. Nakashima, J. Phys. Chem. B 103 (1999) 304–308.
[21] (a) P. Puthiaraj, P. Suresh, K. Pitchumani, Green Chem. 16 (2014) 2865–2875 (and references therein);
(b) A.S. Demir, Ö. Reis, M. Emrullahoglu, J. Org. Chem. 68 (2003) 10130–10134.
[22] D.F. Shriver, M.A. Drezdzon, The Manipulation of Air-sensitive Compounds, Wiley-VCH Publishers, New York, 1986.
[23] R.E. Bachman, K.H. Whitmire, Inorg. Chem. 33 (1994) 2527–2533.
[24] G.J. Kubas, Inorg. Synth. 19 (1979) 90–92.
[25] (a) B.L. Benac, E.M. Burgess, A.J. Arduengo, J. Org. Syn. 64 (1986) 92–96;
(b) H.V. Huynh, T.C. Neo, G.K. Tan, Organometallics 25 (2006) 1298–1302;
(c) K.M. Hindi, T.J. Siciliano, S. Durmus, M.J. Panzner, D.A. Medvetz, D.V. Reddy, L.A. Hogue, C.E. Hovis, J.K. Hilliard, R.J. Mallet, C.A. Tessier, C.L. Cannon,

Please cite this article in press as: M. Shieh, et al., Journal of Organometallic Chemistry (2017), https://doi.org/10.1016/j.jorganchem.2017.10.039

W.J. Youngs, J. Med. Chem. 51 (2008) 1577–1583.

[26] G.M. Sheldrick, SADABS, Bruker AXS Inc., Madison, Wisconsin, USA, 2003.

[27] (a) G.M. Sheldrick, SHELXL97, Version 97-2, University of Gottingen, Germany, 1997;
(b) G.M. Sheldrick, Acta Crystallogr. Sect. A 64 (2008) 112–122.

[28] (a) M.L. Bruce, B.K. Nicholson, A.H. White, J. Organomet. Chem. 240 (1982) C33–C37;
(b) C.-W. Hsu, J.-S.K. Yu, C.-H. Yen, G.-H. Lee, Y. Wang, Y.-C. Tsai, Angew. Chem. Int. Ed. 47 (2008) 9933–9936.

Please cite this article in press as: M. Shieh, et al., Journal of Organometallic Chemistry (2017), https://doi.org/10.1016/j.jorganchem.2017.10.039